Fermi National Accelerator Laboratory

FERMILAB-Conf-93/198-E

CDF

Measurement of the B^+ and B^0 Lifetimes

The CDF Collaboration

Fermi National Accelerator Laboratory
P.O. Box 500, Batavia, Illinois 60510

August 1993

Submitted to the *International Symposium on Lepton and Photon Interactions*,
Cornell University, Ithaca, New York, August 10-15, 1993

Disclaimer

CDF/PUB/BOTTOM/PUBLIC/2153
FERMILAB-CONF-93/198-E

Measurement of the B^+ and B^0 Lifetimes

The CDF Collaboration

Abstract

The lifetimes of the B^+ and B^0 have been measured using a sample of fully reconstructed B decays. Using $\sim 19,000$ $J/\psi \to \mu^+\mu^-$ decays recorded with the Collider Detector at Fermilab, 75 ± 10 charged and 61 ± 9 neutral B mesons have been reconstructed in the CDF silicon vertex detector. Unbinned likelihood fits to the proper lifetime distributions of these B mesons give

$$\begin{aligned} \tau^{\pm} &= 1.63 \pm 0.21\,(\text{stat}) \pm 0.16\,(\text{sys})\ \text{ps} \\ \tau^{0} &= 1.54 \pm 0.22\,(\text{stat}) \pm 0.10\,(\text{sys})\ \text{ps} \\ \tau^{\pm}/\tau^{0} &= 1.06 \pm 0.20\,(\text{stat}) \pm 0.12\,(\text{sys}) \end{aligned}$$

Submitted International Symposium on Lepton and Photon Interactions,
Cornell University, Ithaca, NY, August 10-15, 1993

In the past two years, precision measurements of the average b-flavored hadron lifetime have been performed [1, 2]. The results of these measurements can be used to calculate the Cabibbo-Kobayashi-Maskawa matrix element $|V_{cb}|$ within the context of a model of b meson decay [3]. The simplest such approach is the spectator model, which predicts that the charged and neutral B meson lifetimes should be equal. Although deviations from the spectator model are large in the charm sector, they are expected to be much smaller for b-hadron decays. Calculations of the lifetime ratio that include non-spectator diagrams predict τ^+/τ^0 to be equal to 1.0 within 10-20% [4].

Measurements of the lifetimes of the B^+ and B^0 have been made at PEP and LEP using partially reconstructed decays containing a lepton and a D^0 or $D^{*\pm}$ [5]. Indirect measurements have also been made by CLEO and ARGUS, using the ratio of the B^+ and B^0 semileptonic branching ratios [6]. We present here a measurement of the B^+ and B^0 lifetimes using fully reconstructed decays of the form $B \rightarrow \Psi \mathbf{K}$, where Ψ represents a J/ψ or $\psi(2S)$ and $\mathbf{K}$ represents a $K^{\pm}$, K^0_S, $K^*(892)^0$ or $K^*(892)^{\pm}$. The data used in this analysis were recorded by the Collider Detector at Fermilab (CDF) during the first half of the 1992-1993 Tevatron run. The data sample corresponds to an integrated luminosity of ~ 11 pb^{-1} of $p\bar{p}$ collisions at a center-of-mass energy of 1.8 TeV. Throughout this paper, references to a specific charge state imply the charge-conjugate state as well.

The CDF detector has been described in detail elsewhere [7]. The detector systems used for this analysis are the silicon vertex detector (SVX), the central tracking chamber (CTC) and the muon system. The SVX and CTC are located in a 1.4 T solenoidal magnetic field. The SVX consists of 4 layers of silicon-strip detectors with r-ϕ readout, including pulse height information [8]. The pitch between readout strips is 60 μm and a spatial resolution of 13 μm has been obtained. The first measurement plane is located 2.9 cm from the interaction point, leading to an impact parameter resolution of ~ 15 μm for tracks with $p_T > 5$ GeV/c. The CTC is a cylindrical drift chamber containing 84 layers, which are grouped into alternating axial and stereo superlayers containing 12 and 6 layers respectively. The CTC has a resolution of $\delta p_T/p_T = [(0.0011 p_T)^2 + (0.0066)^2]^{\frac{1}{2}}$ for beam constrained tracks, where p_T is the momentum transverse to the beam direction (measured in GeV/c). The central muon system consists of three detector elements. The Central Muon Chambers (CMU), located behind ~ 5 absorption lengths of material, provide muon identification over 85% of ϕ for the pseudorapidity range $|\eta| \leq 0.6$, where $\eta = -\ln[\tan(\theta/2)]$. This η region is further instrumented by the Central Muon Upgrade (CMP), located after ~ 8 absorption lengths. The central muon extension (CMX), which covers the pseudorapidity range $0.6 < |\eta| < 1.0$, provides muon identification over 67% of the azimuth and is located behind ~ 6 absorption lengths.

CDF uses a three-level trigger system. At Level 1, two-muon candidates are selected with a trigger that requires the presence of 2 charged tracks in the central muon system. The efficiency for finding a muon at Level 1 rises from 50% at $p_T = 1.8$ GeV/c to 90% for $p_T = 3.8$ GeV/c. At Level 2, the dimuon trigger requires that at least one of the muon tracks match a charged track in the CTC. This CTC track is found by a Central Fast Track processor (CFT) [9]. The efficiency to find a track in

the CFT rises from 50% at 2.7 GeV/c to 90% for p_T = 3.4 GeV/c. At Level 3, the trigger (which is implemented using online track reconstruction software) selects J/ψ candidates by requiring the presence of two oppositely charged muons with invariant mass between 2.8 and 3.4 GeV/c^2 [10].

To reduce the background in the sample obtained with this trigger, the following muon selection cuts were applied: 1) The distance between the track in the muon chamber and the extrapolated CTC track was calculated in the transverse plane. The difference was required to be less than 3.0 standard deviations (σ) from zero, where σ is calculated as the quadratic sum of the multiple scattering and measurement errors. For muons in the CMU, where z position information is available, the 3σ matching requirement is made in the longitudinal view as well. 2) The energy deposited in the hadronic calorimeter by each muon was required to be greater than 0.1 GeV, corresponding to the presence of a minimum ionizing track. 3) The reconstructed p_T of at least one of the muon tracks was required to be > 2.5 GeV/c.

Figure 1 shows the invariant mass distribution for oppositely charged dimuon candidates obtained with these cuts and with the additional requirement that both muons be reconstructed in the SVX. The invariant mass here has been calculated after constraining the two tracks to come from a common point in space ("vertex constraint"). The arrows, placed ± 80 MeV/c^2 from the world average value of the J/ψ mass, indicate the mass cuts applied to define J/ψ candidates. The total number of events in the signal region is 22,894. The number of J/ψ events after background subtraction is 19849 ± 162.

Using this J/ψ sample, we have searched for the decay $\psi(2S) \rightarrow J/\psi\pi^+\pi^-$. To improve the mass resolution, the four tracks are vertex constrained and the dimuon mass is simultaneously constrained to the world average J/ψ mass. Combinations where the χ^2 of this fit corresponds to a confidence level of less than 1% are rejected. Combinatoric background is further reduced by requiring that the two pions have an invariant mass of less than 600 MeV/c^2 and requiring that the $\psi(2S)$ have $p_T > 3.0$ GeV/c. Figure 2 shows the invariant mass distribution of the $J/\psi\pi^+\pi^-$ combinations. The $\psi(2S)$ candidates are defined as all the combinations having a mass within ± 20 MeV/c^2 of the world average $\psi(2S)$ mass, as indicated by the arrows on the figure.

We search for B mesons in the following channels:

$$
\begin{array}{lcll}
B^+ & \rightarrow & J/\psi\ K^+ & \rightarrow\ \mu^+\mu^- K^+ \\
B^+ & \rightarrow & J/\psi\ K^*(892)^+ & \rightarrow\ \mu^+\mu^- K^0_S\pi^+ \\
B^+ & \rightarrow & \psi(2S)\ K^+ & \rightarrow\ \mu^+\mu^-\pi^+\pi^- K^+ \\
B^+ & \rightarrow & \psi(2S)\ K^*(892)^+ & \rightarrow\ \mu^+\mu^-\pi^+\pi^- K^0_S\pi^+ \\
B^0 & \rightarrow & J/\psi\ K^0_S & \rightarrow\ \mu^+\mu^- K^0_S \\
B^0 & \rightarrow & J/\psi\ K^*(892)^0 & \rightarrow\ \mu^+\mu^- K^+\pi^- \\
B^0 & \rightarrow & \psi(2S)\ K^0_S & \rightarrow\ \mu^+\mu^-\pi^+\pi^- K^0_S \\
B^0 & \rightarrow & \psi(2S)\ K^*(892)^0 & \rightarrow\ \mu^+\mu^-\pi^+\pi^- K^+\pi^-
\end{array}
$$

To insure that the decay point of the B meson is well measured, the following quality cuts are applied to all tracks used in the reconstruction of the B meson: 1) Each track must contain at least 2 CTC axial superlayers each of which must have at least 5 hit layers. 2) Each track must contain at least 2 CTC stereo superlayers each of which

must have at least 2 hit layers. 3) Each track must be reconstructed in the SVX with hits on at least 2 out of 4 possible layers. For tracks with only 2 SVX hits, the contribution of the SVX hits to the track χ^2 must be less than 8. Requirement 3 is not imposed on the tracks used to reconstruct K^0_S candidates since the decay point of the K^0_S may be outside the SVX outer radius. These K^0_S candidates are selected by requiring two oppositely charge tracks (assumed to be pions) with impact parameters with respect to the primary vertex of at least 2 σ, where σ is the quadratic sum of the measurement error on the impact parameter and the size of the beam spot. Figure 3 shows the invariant mass distribution of these $\pi^\pm\pi^\mp$ combinations after a vertex constrained fit and after requiring the impact parameter with respect to the J/ψ vertex be less then 0.2 cm. Combinations with a mass more than 20 MeV/c^2 from the world average K^0_S mass are rejected.

Reconstruction of the B candidates proceeds in the same manner as the $\psi(2S)$. A J/ψ or $\psi(2S)$ candidate is combined with a track (assumed to be a $K^\pm$), with a K^0_S candidate, with two oppositely charged tracks (assumed to be a $K^\pm$ and a $\pi^\mp$) forming a $K^*(892)^0$ candidate or with a K^0_S candidate plus a track (assumed to be a $\pi^\pm$) forming a $K^*(892)^\pm$ candidate. The J/ψ and $\psi(2S)$ candidates are mass constrained and all tracks (except the K^0_S decay products) are vertex constrained. If the combination of tracks includes a K^0_S candidate, a second fit is used to vertex and mass constrain the K^0_S decay products. Each vertex fit is required to have a χ^2 which corresponds to a confidence level of better than 1%. Combinations where the $K^*(892)$ mass is more than 80 MeV/c^2 from the world average mass are rejected.

Final kinematic cuts for the reconstruction of the $B^\pm$ and B^0 have been optimized to give the smallest statistical error on the background subtracted B meson signals. For this optimization, a Monte Carlo simulation was used to model the signal coming from B meson decays. Data in the sidebands of the invariant mass distributions were used to determine the number of background events. The optimization was done separately for each channel, but the final cuts are not strongly decay-mode dependent. For simplicity, we have chosen to use the same selection criteria for all channels: $p_T(B) > 6.0$ GeV/c and $p_T(\mathbf{K}) > 1.25$ GeV/c. Here $p_T(\mathbf{K})$ is the transverse momentum of the reconstructed $K^\pm$, $K^*(892)$, or K^0_S candidate. No p_T cuts are placed on the individual tracks used to reconstruct the $\mathbf{K}$ decay.

The reconstruction described above has been applied to all possible track combinations, thus allowing the same J/ψ to be used for more than one B candidate. Since such duplicate events could bias the lifetime measurement, they have been removed as follows. We consider all candidates meeting the above cuts and with total mass within ± 120 MeV/c^2 of the world average B mass. For events where the same J/ψ is used with more than one combination of additional tracks, we keep only the candidate with the highest confidence level obtained from the χ^2 of the vertex-constrained fit. For events where the duplicate candidates arise from the ambiguity of the mass assignment for the two tracks forming the $K^*(892)^0$, the two candidates will have identical vertex χ^2. Here we keep only the candidate with the $K\pi$ or πK mass assignment closest to the world average $K^*(892)^0$ mass. The effect of the duplicate removal is to decrease the number of events in the peak region by $\sim 10\%$.

Background in the B meson invariant mass distributions comes from combinations

of J/ψ's with tracks produced during the b-quark fragmentation or with other remanents of the $p\bar{p}$ collision. Such tracks should reconstruct to the primary vertex. Thus the background is largest for events where the decay distance is small. Although the fit to the B meson lifetimes will use data with all proper times, a good estimate of the statistical power of the data can be obtained by studying the number of signal events in the sample with proper decay length greater than 100 μm. Figures 4a and 5a show the invariant mass distributions all $B^{\pm}$ and B^0 candidates. Figures 4b and 5b show the same distributions once the 100 μm requirement is applied. The cut on proper time removes a good fraction of the background.

We define the B meson signal region to be those events with invariant mass within ± 30 MeV/c^2 of the world average B meson mass. Sideband regions, used to determine the shape of the background under the mass peak, are defined to have invariant mass between 60 and 120 MeV/c^2 from the world average B mass. These sidebands have been chosen to exclude the regions where $B \rightarrow \Psi \mathrm{K} X$ events are kinematically allowed.

The technique used to measure the B^+ and B^0 lifetimes is similar to that used to measure the average B lifetime [2]. For each B candidate, the two dimensional decay distance L_{xy} is calculated. L_{xy} is the projection of the vector $\vec{X}$ pointing from the primary to the secondary vertex onto the transverse momentum of the B candidate:

$$L_{xy} \equiv \frac{\vec{X} \cdot \vec{p_T}^B}{|\vec{p_T}^B|}$$

The primary vertex position is approximated by the mean beam position, determined run-by-run using SVX information and averaging over many events. The transverse profile of the beam is circular and has an rms of ~ 40 μm. Since the momentum of the B meson is known, the proper decay length $c\tau$ can be determined:

$$c\tau = L_{xy} \frac{M_B}{p_T{}^B}$$

The lifetime of the $B^{\pm}$ and B^0 are obtained by performing separate unbinned maximum likelihood fits to the $c\tau$ distributions of the charged and neutral event samples. For each sample, the signal and sideband distributions are fit simultaneously. During this fit the number of background events in the peak region is constrained to be equal, within Poisson fluctuations, to the number of events in the normalized sideband distributions. The fit is performed under the following assumptions:

- The signal region contains both signal events (i.e. real B mesons correctly reconstructed) and background events. The proper times of the signal events are distributed according to an exponential function convoluted with a Gaussian resolution function. The slope of the exponential (λ) is the lifetime to be measured. The Gaussian resolution is determined for each event from the measurement error on L_{xy}. The fit parameter α gives the fraction of signal events in the peak region while $\mathcal{N}$ gives the number of signal events.

- Background events in the signal region have the same $c\tau$ distribution as the events in the sideband region. The proper times of the background and sideband

Parameter		Fit results					
		Charged B			Neutral B		
$\lambda = c\tau$	[μm]	488	$\pm$	63	462	$\pm$	67
α	[%]	33	$\pm$	3	18	$\pm$	2
$\mathcal{N}$	[events]	75	$\pm$	10	61	$\pm$	9
f^-	[%]	6	$\pm$	4	1	$\pm$	1
λ^-	[μm]	38	$\pm$	15	134	$\pm$	87
f^+	[%]	5	$\pm$	2	10	$\pm$	2
λ^+	[μm]	154	$\pm$	50	86	$\pm$	13
Lifetime ratio $= \tau^\pm/\tau^0 = 1.06 \pm 0.20$							

Table 1: Results of the Fits to the $B^\pm$ and B^0 Lifetime.

events are distributed according to the the sum of a Gaussian resolution function and two exponential tails, one above the Gaussian and one below, each with a different slope. This functional form of the background is identical to that used in Reference [2]. The fit parameters f^+ and f^- are the fraction of background events in the positive-side and negative-side exponentials, while λ^+ and λ^- are the exponential slopes.

Figure 6a and b show the distribution in $c\tau$ of the signal and sideband regions respectively for all $B^\pm$ candidates. Figure 7a and b show the same distributions for the B^0. The curves show the results of the maximum likelihood fit to the data. The results of these fits are also summarized in Table 1. The fitted lifetimes are:

$$\begin{aligned} \tau^\pm &= 1.63 \pm 0.21 \text{ ps} \\ \tau^0 &= 1.54 \pm 0.22 \text{ ps} \end{aligned}$$

where the quoted errors are are statistical only, but include correlations between the fit parameters.

Estimates of the systematic uncertainty on the lifetime measurements are listed in Table 2. Possible bias in the lifetime measurements due to residual misalignment, trigger bias and movement of the beam-spot within a single run are derived in the same manner as for the inclusive b-hadron lifetime measurement [2] and are small when compared to the statistical uncertainties on the lifetimes of the B^+ and B^0. Since the result of the maximum likelihood fit depends on the decay-length error calculated for each event, we have varied these errors by an overall scale factor and studied the result of this variation on the fitted lifetime. This introduces a 10 μm uncertainty in the proper decay length. From studies using event samples generated with a Monte Carlo technique, we place the systematic uncertainty due to biases in the fitting procedure at 5 μm.

The largest systematic uncertainty on this measurement comes from the presence of a small number of events in the positive lifetime tails of the sideband distributions. These events are not well modeled by our background shape (Gaussian plus positive

Source	Error on $B^{\pm}$ (μm)	Error on B^0 (μm)
Residual Misalignment	10	10
Trigger Bias	6	6
Beam Stability	5	5
Uncertainty in $c\tau$ Resolution	10	10
Possible Bias in the Fit Procedure	5	5
Uncertainty in Sideband Shape	45	25
Total	48	30

Table 2: Summary of Systematic Uncertainties

and negative going exponentials). The estimated contribution of such events to the $c\tau$ distribution in the signal region is 3.5 events in the $B^{\pm}$ case and 1.5 events in the B^0 case. To determine the bias these tails could introduce, we have fit the lifetime using an extreme model of the background shape. We add to the background parameterization a flat component in the range $0 < c\tau < 0.2$ cm. The normalization of this flat component is allowed to vary in the fit. For the B^+ case, the likelihood fit places 3% of the events in the flat background distribution. The B^+ lifetime changes from 488 μm to 449 μm. For the B^0 case, the likelihood fit places 1% of the events in the flat background distribution. The B^0 lifetime changes from 462 μm to 441 μm. Based on these results, we estimate a systematic uncertainty of 45 μm on the $B^{\pm}$ lifetime and 25 μm on the B^0 lifetime. When calculating the uncertainty on the lifetime ratio, we assume that these uncertainties on the charged and neutral lifetimes are uncorrelated.

In conclusion, we have measured the lifetimes of the B^+ and B^0 mesons using a sample of fully reconstructed B meson decays in a variety of modes containing a $J/\psi \rightarrow \mu^+\mu^-$ in the decay chain. We find

$$\begin{aligned} \tau^{\pm} &= 1.63 \pm 0.21\ (\text{stat}) \pm 0.16\ (\text{sys})\ \text{ps} \\ \tau^{0} &= 1.54 \pm 0.22\ (\text{stat}) \pm 0.10\ (\text{sys})\ \text{ps} \\ \tau^{\pm}/\tau^{0} &= 1.06 \pm 0.20\ (\text{stat}) \pm 0.12\ (\text{sys}) \end{aligned}$$

The measurement presented is based on $\sim 1/2$ of the data currently collected by CDF.

We thank the CDF technical support staff at all CDF institutions for their hard work and dedication. We also thank the Fermilab Accelerator Division for their hard and successful work in commissioning the machine for this physics run. This work was supported by the Department of Energy; the National Science Foundation; the Istituto Nazionale di Fisica Nucleare, Italy; the Ministry of Science, Culture, and Education of Japan; the Natural Sciences and Engineering Research Council of Canada; and the A. P. Sloan Foundation.

References

[1] P. Abreu et al., Z. Phys. C 53 (1992) 567; B. Adeva et. al. Phys. Lett B 270 (1992) 111; P.D. Acton et al., Phys. Lett. B 274 (1992) 513; D. Buskulic, et al., Phys. Lett. B 295 (1992) 174; P.D. Acton et al., CERN-PPE/93-92, submitted to Z. Phys. C.

[2] F. Abe et al., FERMILAB-PUB-93/158-E, submitted to Phys. Rev. Lett.

[3] N. Cabbibo and L. Maiani, Phys. Lett. B 19 (1978) 109; M. Suzuki, Nucl. Phys. B 145 (1978) 420; A. Ali and E. Pietarinen, Nucl. Phys. B 145 (1979) 519.

[4] M.B. Voloshin and M.A. Shifman, Sov. Phys. JETP 64 (1986) 698; G. Altarelli, S. Petrarca, Phys. Lett. B 261 (1991) 303; I. Bigi and N. Uraltsev, Phys. Lett. B 280 (1992) 271.

[5] S. Wagner, et al., Phys. Rev. Lett. 64 (1990) 1095; P. Abreu, et al., Z. Phys. C 57 (1993) 181; B. Buskulic, et al., Phys. Lett B 297 (1992) 449; D. Buskulic et. al,, CERN PPE/93-42, to be published in Physics Letters B; P.D. Acton et. al, CERN-PPE/93-33.

[6] B. Albrecht, et al., Phys. Lett. B 275 (1992) 195; R. Fulton, et al., Phys. Rev. D43 (1991) 236; D.S. Akerib, et al., *A Measurement of the Charged and Neutral B Meson Lifetime Ratio*, contributed paper to the XXVI International Conference on High Energy Physics, August 1992, Dallas, Texas.

[7] F. Abe et al., Nucl. Inst. and Meth. A271 (1988) 387 and references therein.

[8] D. Amidei et. al., Nucl. Inst. and Meth. A 289 (1990) 388; O. Schneider et. al., Proceedings of the 7th Meeting of the American Physical Society, Division of Particles and Fields, Fermilab, Nov 1992, World Scientific Press, 1743.

[9] G.W. Foster et. al., Nucl. Inst. and Meth. A 269 (1988) 93.

[10] J. T. Carroll et al. Nucl. Inst. and Meth. A300 (1991) 552.

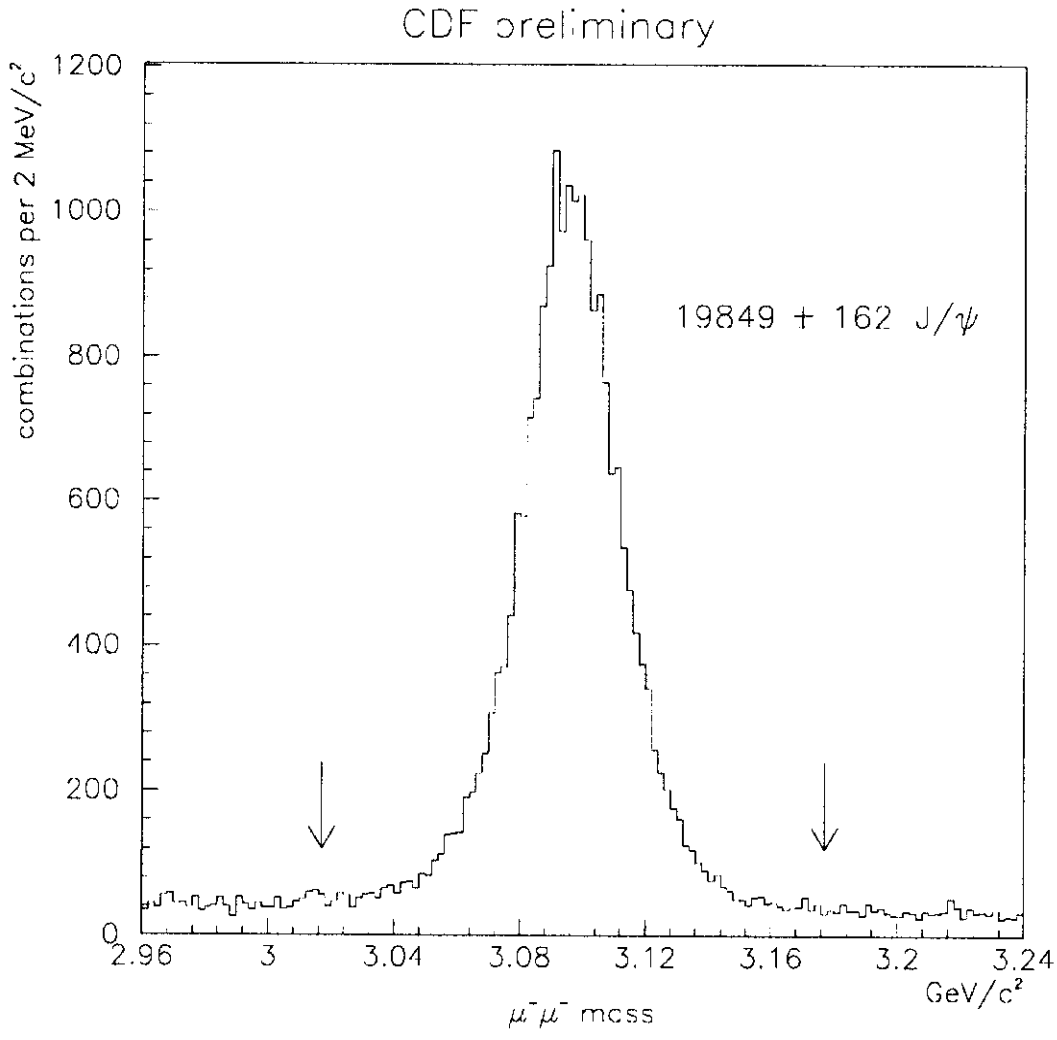

Figure 1: The invariant mass distribution of $\mu^+\mu^-$ pairs. The two muons are required to be reconstructed in the SVX and to come from a common vertex. The arrows, placed at ± 80 MeV/c^2 around the world average J/ψ mass, indicate the mass cuts applied to define the J/ψ sample.

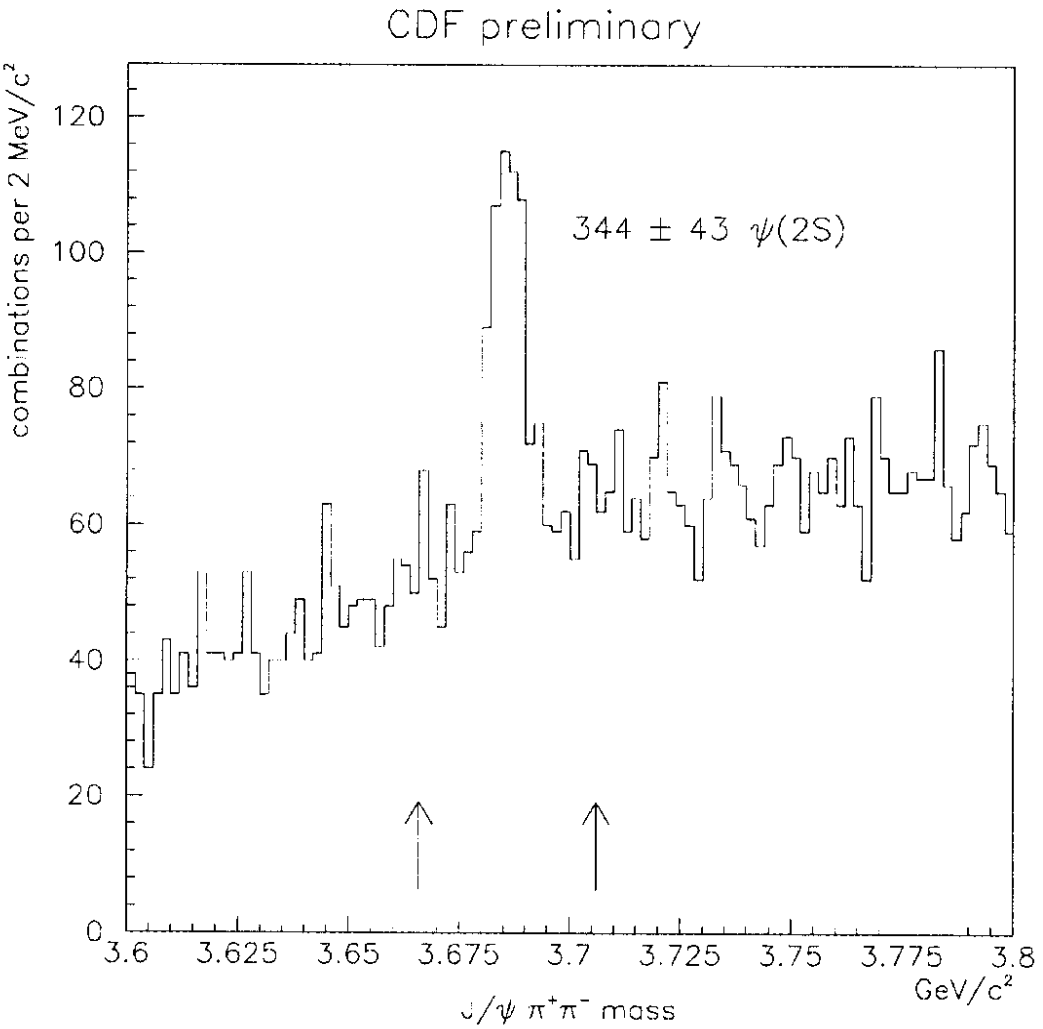

Figure 2: The invariant mass distribution of all $J/\psi\ \pi\pi$ combinations meeting the requirements described in the text. The 4 tracks are required to come from a common vertex, and the $\mu^+\mu^-$ invariant mass is constrained to the J/ψ mass. The arrows, placed at ± 20 MeV/c^2 from the world average $\psi(2S)$ mass, indicate the mass cuts applied to define the $\psi(2S)$ sample.

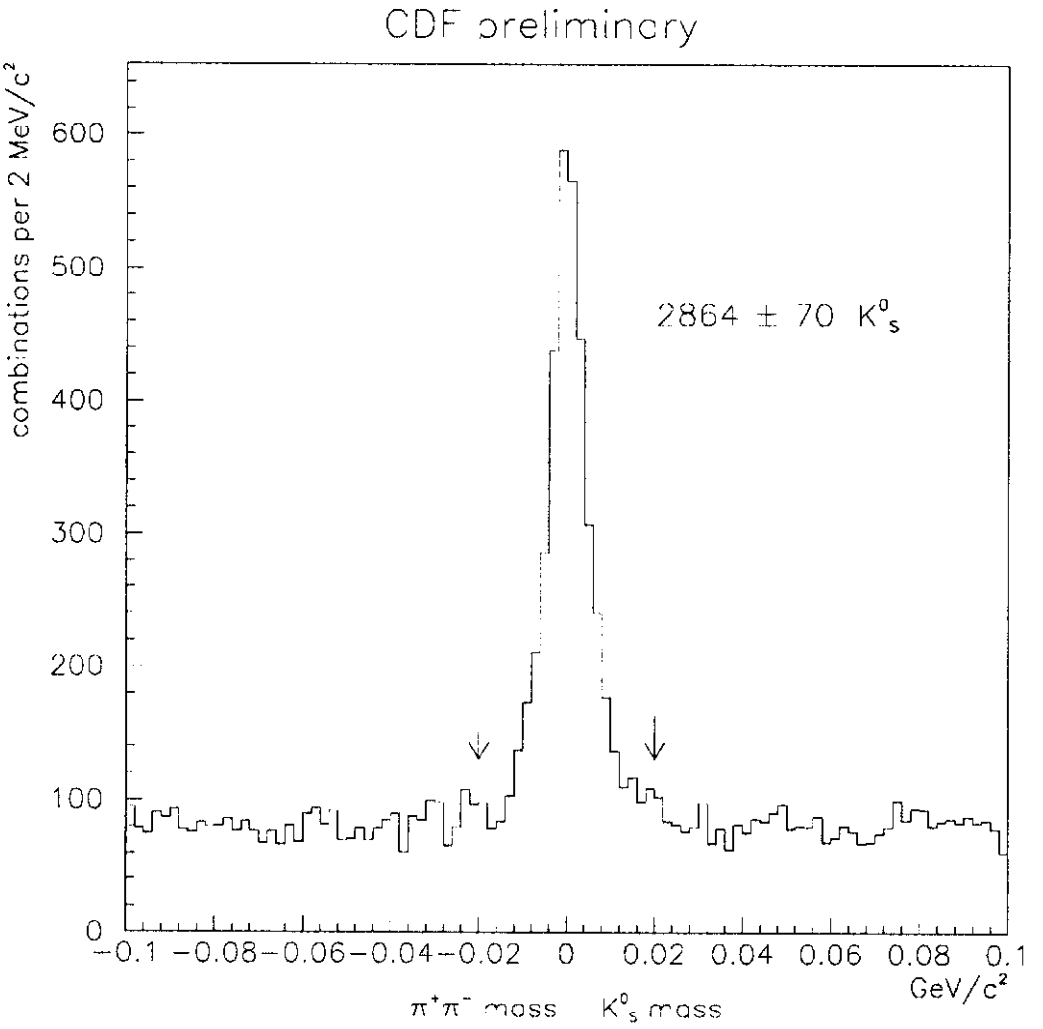

Figure 3: The invariant mass distribution of all $\pi^+\pi^-$ pairs that form K^0_S candidates. The quantity shown is the $\pi\pi$ mass minus the world-average K^0_S mass. The arrows, placed at ± 20 MeV/c^2 indicate the mass cuts applied to define the K^0_S sample.

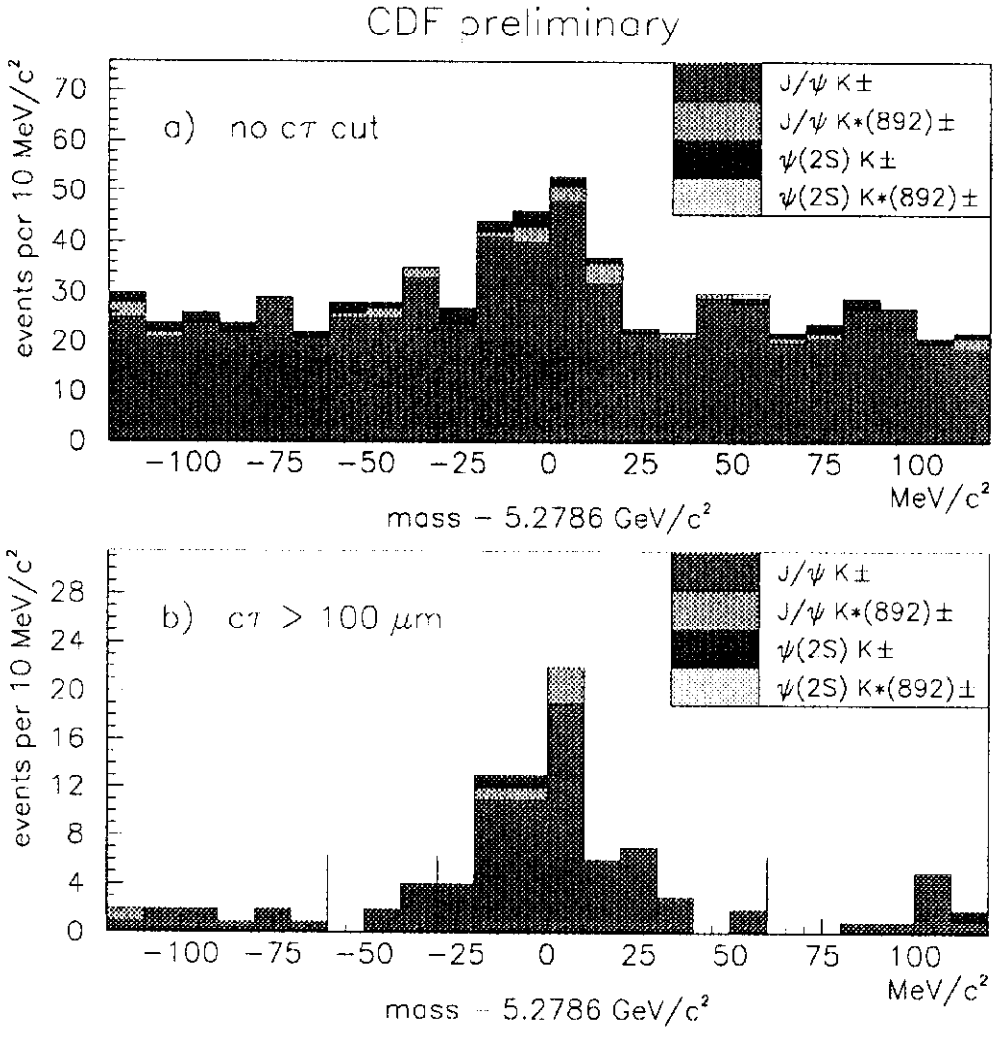

Figure 4: The invariant mass distribution for all reconstructed $B^{\pm}$ mesons. The quantity shown is the measured mass minus the world average B-meson mass (5.2786 GeV/c^2). a) All events passing the selection described in the text. b) The subset of events with the proper decay length $c\tau > 100\ \mu m$. In the fit to the lifetime, the peak region is defined as the 6 central bins. The sideband regions are defined as the 6 leftmost and the 6 rightmost bins.

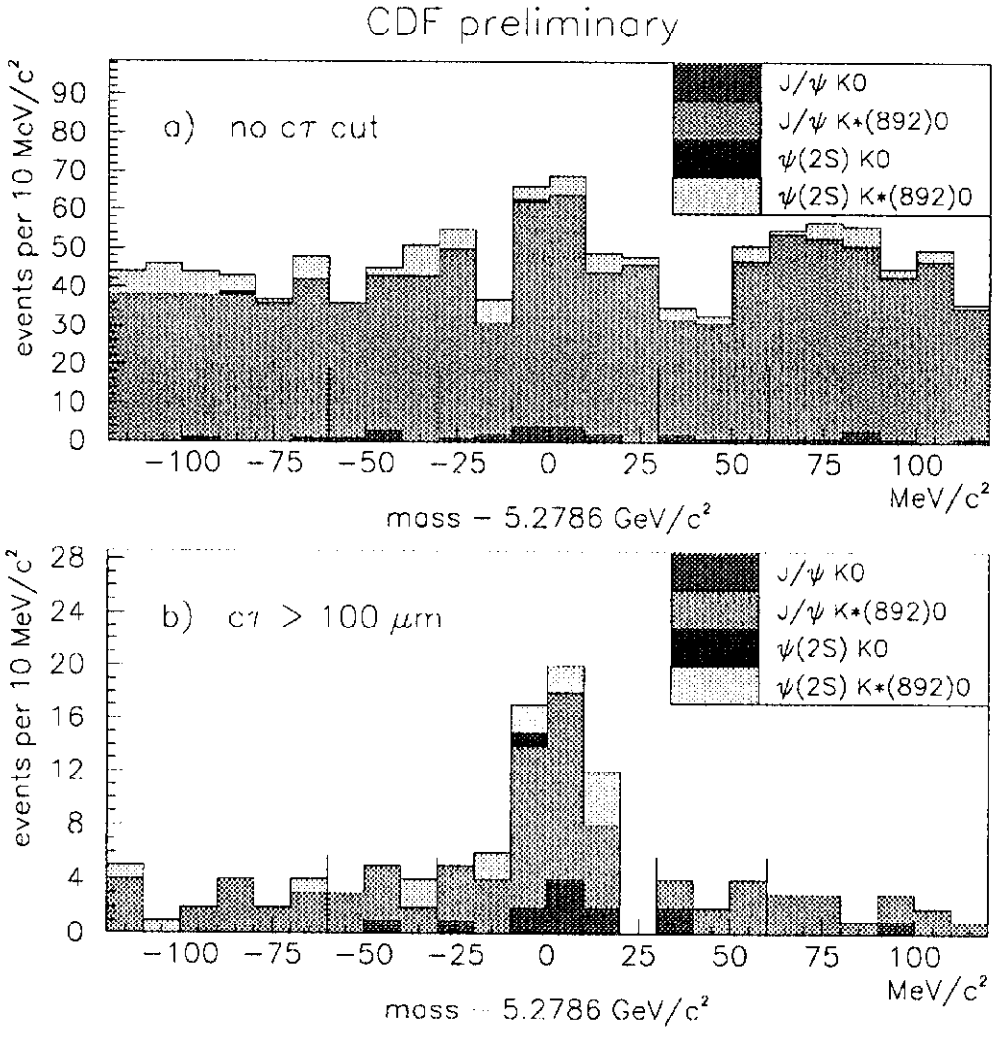

Figure 5: The invariant mass distribution for all reconstructed B^0 mesons. The quantity shown is the measured mass minus the world average B meson mass (5.2786 GeV/c^2). a) All events passing the selection described in the text. b) The subset of events with the proper decay length $c\tau > 100\ \mu m$. In the fit to the lifetime, the peak region is defined as the 6 central bins. The sideband regions are defined as the 6 leftmost and the 6 rightmost bins.

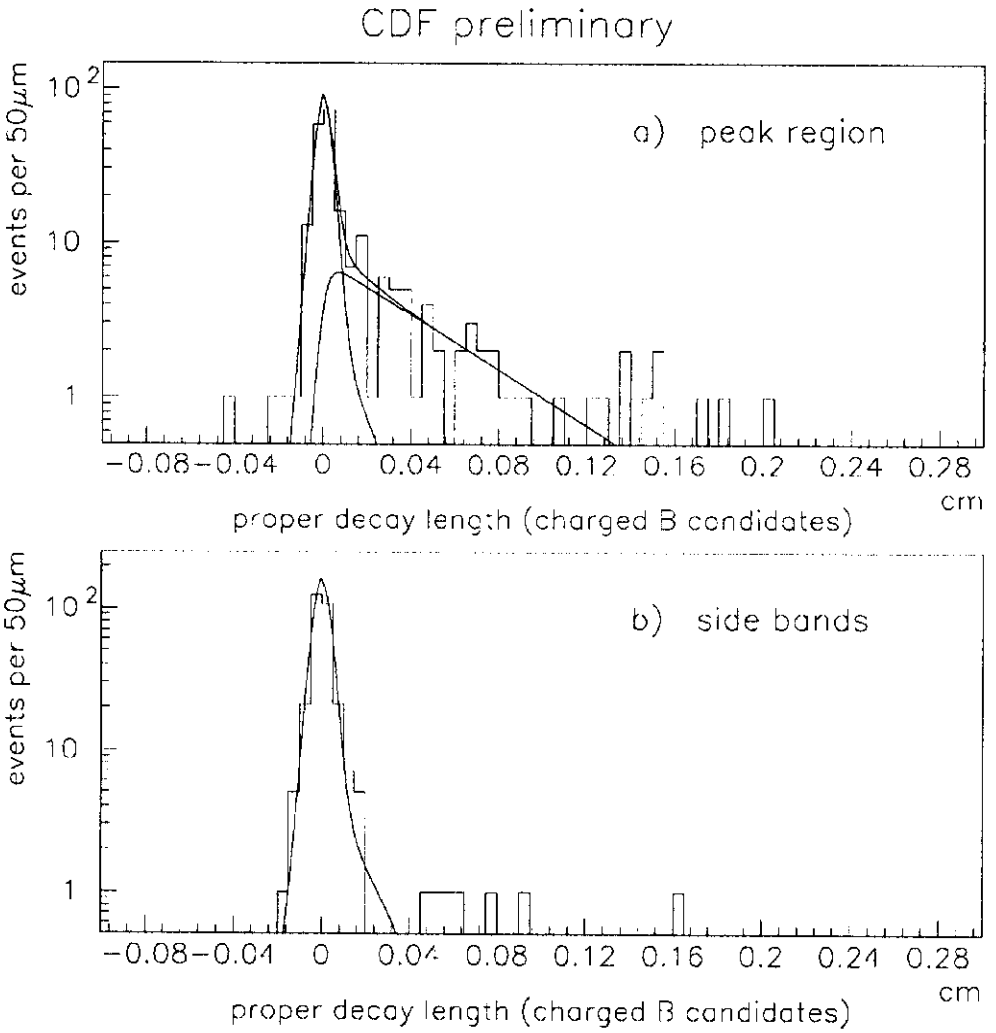

Figure 6: Fit of the $c\tau$ distributions of all reconstructed $B^{\pm}$ mesons. The 3 curves superimposed on the $c\tau$ distribution of the peak region events (shown on top) are the contributions from the signal, the background, and their sum, as determined from the likelihood fit described in the text. The curve superimposed on the $c\tau$ distribution of the sideband events (shown on bottom) is the result of the same fit.

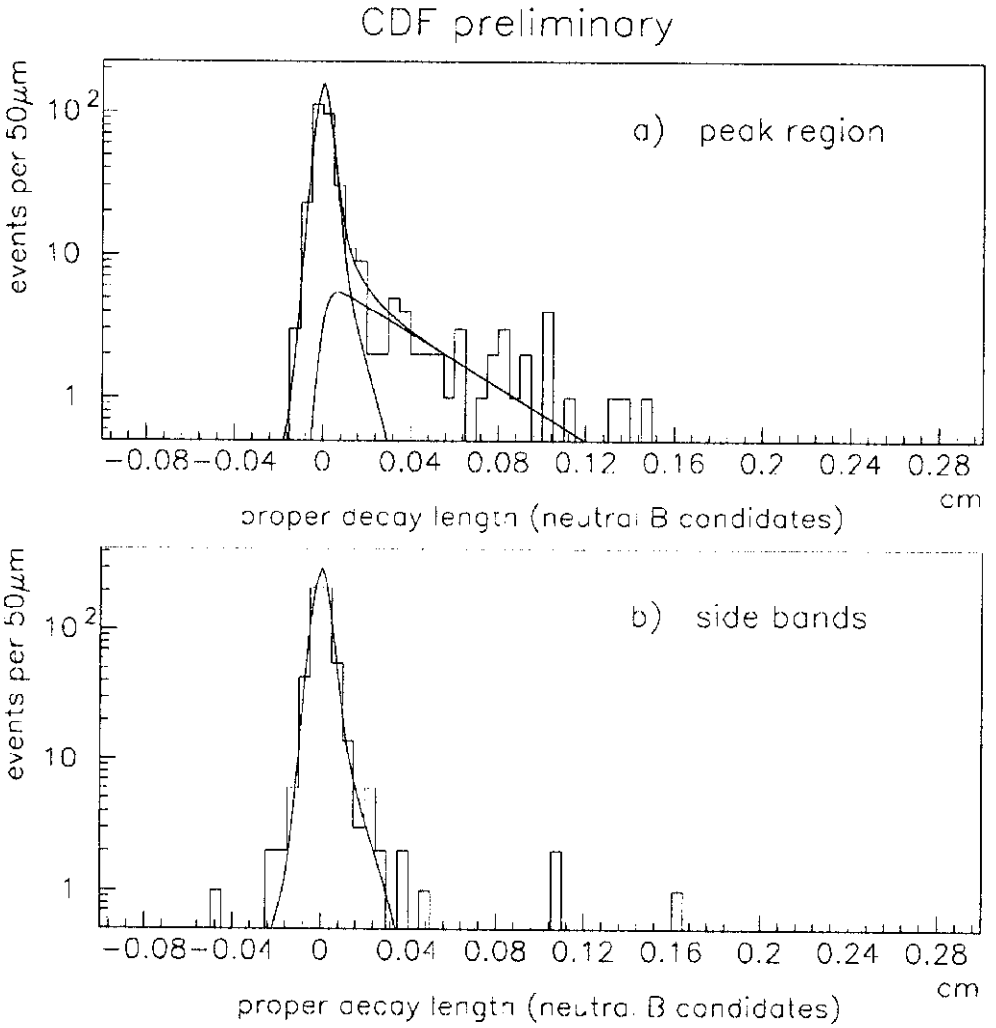

Figure 7: Fit of the $c\tau$ distributions of all reconstructed B^0 mesons. The 3 curves superimposed on the $c\tau$ distribution of the peak region events (shown on top) are the contributions from the signal, the background, and their sum, as determined from the likelihood fit described in the text. The curve superimposed on the $c\tau$ distribution of the sideband events (shown on bottom) is the result of the same fit.